Available online at www.sciencedirect.com
ScienceDirect
Journal of the European Ceramic Society 29 (2009) 2873–2883
www.elsevier.com/locate/jeurceramsoc

Carbon-rich SiCN ceramics derived from phenyl-containing poly(silylcarbodiimides)

Gabriela Mera[a,*], Ralf Riedel[a], Fabrizia Poli[b], Klaus Müller[b,c,d]

[a] *Technische Universität Darmstadt, Institut für Materialwissenschaft, Petersenstrasse 23, D-64287 Darmstadt, Deutschland, Germany*
[b] *Universität Stuttgart, Institut für Physikalische Chemie, Pfaffenwaldring 55, D-70569 Stuttgart, Deutschland, Germany*
[c] *Dipartimento di Ingegneria dei Materiali e Tecnologie Industriali, Universitá degli Studi di Trento, via Mesiano 77, I-38100, Trento, Italy*
[d] *INSTM, UdR Trento, Italy*

Received 28 January 2009; received in revised form 25 March 2009; accepted 26 March 2009
Available online 29 April 2009

Abstract

Novel phenyl-containing polysilylcarbodiimides were synthesized and their thermolysis and crystallization behavior up to 2000 °C was investigated. The Si/C ratio of the preceramic polymer was varied in a defined way by starting from dichlorosilanes with different organic substituents, namely R and R′ with R = phenyl and R′ = H, phenyl, methyl or vinyl. Several techniques were employed to study the structural features of the polymers and their thermolysis products. The temperature of crystallization depends on the carbon content of the precursors. Thus, in the sample with the highest carbon content the separation of β-SiC from the amorphous SiCN matrix is observed at $T > 1500$ °C, resulting in the highest temperature of thermal stability against crystallization ever reported for a SiCN ceramic derived from polysilylcarbodiimides. Moreover, no crystallization of β-Si_3N_4 was observed.

Keywords: Precursors-organic; Spectroscopy; Thermal properties; Carbon; C-rich SiCN ceramics

1. Introduction

Polymer-derived ternary SiCN ceramics are a new class of materials possessing oxidation and creep resistance up to exceptionally high temperatures,[1,2] properties which are improved when the ceramics are fabricated with a high content of excess carbon, as published recently in the case of SiCO materials.[3–5] The high-temperature stability was also traced back to the presence of nanodomains with 1–3 nm in size as shown recently by SAXS measurements of polymer-derived ceramics (PDC) with low carbon content.[6]

A main feature of polymer-derived ceramics is their possibility to incorporate free carbon into the microstructure. This issue has been addressed in several publications where primarily PDCs of low free carbon content were considered.[1,7,8] Until recently it was assumed that an excess of carbon is detrimental to the mechanical and electrical properties as well as to the oxidation resistance of such ceramics. This view has been completely revised, since studies on SiCO–carbon hybrids showed a much higher stability against crystallization and high-temperature resistance to oxidation than originally anticipated.[9,10] It was also reported that carbon-rich PDCs retain their amorphous character to higher temperatures than the carbon-poor PDC analogues.[11] Based on these investigations, it was concluded that the presence of carbon is essential for the inhibition of crystallization and lowering the carbothermal reactivity.

Polysilylcarbodiimides represent an important class of precursors for SiCN ceramics which are thermally more stable than the analogous polysilazanes.[1,2,12,13] They are known to form two amorphous phases, namely Si_3N_4 and free carbon, at about 1000 °C, as can be demonstrated, for instance, by solid-state NMR studies.[14] However, until now there have been no reports about carbon-rich SiCN ceramics obtained from thermolysis of polysilylcarbodiimides.

For this reason, we synthesized several phenyl-substituted polysilylcarbodiimides, which after thermolysis are expected to yield SiCN ceramics containing a substantial amount of free carbon. Klebe and Murray reported the synthesis of

* Corresponding author. Tel.: +49 6151 166340; fax: +49 6151 166346.
E-mail address: mera@materials.tu-darmstadt.de (G. Mera).

0955-2219/$ – see front matter © 2009 Elsevier Ltd. All rights reserved.
doi:10.1016/j.jeurceramsoc.2009.03.026

diphenyl-substituted polysilylcarbodiimide for the first time in 1967[15] followed by Kumar and Shankar in 2002 who obtain a mixture of cyclic silylcarbodiimides and cyclosilazanes.[16]

In the current work, the novel phenyl-substituted polysilylcarbodiimides have an identical substituent R^1 = phenyl. The carbon content in these materials is varied by the second substituent, R^2, which is either a phenyl ring (sample S1), a methyl group (S2), a hydrogen atom (S3) or a vinyl group (S4). Thus, from a comparative study of samples S1–S4 it is possible to examine the effect of the carbon content on both the structural evolution during thermolysis and the properties of the resulting SiCN ceramics. In this context, the precursor polymers, the intermediates during thermolytic conversion and the resulting SiCN ceramics are thoroughly characterized by means of several spectroscopic methods, X-ray diffraction and related techniques.

2. Experimental procedure

2.1. Chemicals

Dichlorodiphenylsilane, dichlorophenylsilane, dichloromethylphenylsilane, dichlorovinylphenylsilane, dichlorodimethylsilane and pyridine were purchased from Sigma–Aldrich Chemie GmbH, Germany. All chemicals were used as received without further purification. Bis(trimethylsilyl)carbodiimide was synthesized according to the literature.[17]

2.2. Synthesis and thermolysis

All reactions were carried out in purified argon atmosphere using standard Schlenk techniques.[18] Bis(trimethylsilyl) carbodiimide (0.047 mol) was mixed under stirring with a catalytic amount of pyridine (0.024 mol). Afterwards, the substituted dichlorosilane (0.047 mol) was added and the reaction mixture was kept under reflux at 66 °C for 6 h (respectively 44 °C for S3, b.p. ($PhHSiCl_2$) = 65–66 °C) and then at 120 °C for another 12 h. The formation of the substituted polysilylcarbodiimide was monitored by means of high-resolution ^{29}Si NMR spectroscopy. After completion of the reaction, the by-product trimethylchlorosilane was removed by distillation.

For the thermolysis of the samples up to 1100 °C, 1–2 g of the polymeric precursor was filled in a quartz crucible. The crucible was then put in a quartz tube, and heated under a steady flow of purified argon (50 mL/min) in a programmable horizontal tube furnace. For the thermolysis below 1600 °C, the samples were first heated to the desired thermolysis temperature with a heating ramp of 100 °C/h. Afterwards, the samples (∼0.5 g) were placed in BN crucibles and were heated in an Astro furnace with a heating ramp of 5 °C/min to the required thermolysis temperature, at which they were kept for 2 h. The thermolysis was completed by cooling the samples to room temperature with a cooling ramp of 10 °C/min. For the thermolysis at higher temperatures (up to 2000 °C), the samples were in a first step thermolyzed at 1100 °C following the procedure described above.

2.3. Characterization techniques

X-ray diffractograms of our samples were measured by a STOE X-ray diffractometer using Ni-filtered Cu Kα radiation at a scan speed of 1° min^{-1}.

FT-IR spectra were recorded on a Nicolet Nexus 470 FTIR spectrometer with a nitrogen-purged optical bench (Nicolet, Madison, WI) equipped with a DTGS detector.

Chemical analysis of the polymers was carried out at Mikroanalytisches Labor Pascher (Remagen/Germany). For the ceramics, the determination of carbon in the ceramic product was measured by a carbon analyzer (CS 800, Eltra GmbH, Neuss). The oxygen and nitrogen content of the powdered ceramic sample was determined by an N/O analyzer (Leco, Type TC-436).

Thermal gravimetric analysis of the polymers was performed on a Netzsch STA 429 apparatus (Selb, Germany). The samples were heated to 1400 °C at a rate of 5 °C/min in argon atmosphere, while simultaneously measuring the mass loss and the gaseous decomposition products via mass spectrometry (Quadrupole Mass Spectrometer).

Raman spectra were recorded on a confocal Horiba HR800 micro-Raman spectrometer by using an excitation laser wavelength of 514.5 nm. For the evaluation of free carbon cluster size in ceramics, Gaussian–Lorentzian curve fitting of the Raman bands (LabSpec 5.21.08 Software) was applied.

Solid-state ^{29}Si NMR experiments were performed on a Varian InfinityPlus 400 NMR spectrometer operating at a static magnetic field of 9.39 T (^{29}Si frequency: 79.46 MHz), while solid-state ^{13}C NMR measurements were carried out on a Bruker CXP 300 spectrometer operating at 7.05 T (^{13}C frequency: 75.47 MHz). All measurements were done by using 4 mm magic angle spinning (MAS) probes. ^{29}Si and ^{13}C NMR spectra were recorded using single pulse, cross-polarization (CP) and ramped cross-polarization (RAMP-CP) excitation.[19] For the ^{29}Si single pulse experiments a pulse angle of 45° (1.75 μs) and a recycle delay of 45 s was used. ^{29}Si RAMP-CP experiments were acquired with a contact time of 5 ms and a recycle delay of 5 s. ^{13}C single pulse experiments were performed using a π/2 pulse length of 4 μs and a recycle delay of 15 s, while for the CP experiments a contact time of 5 ms and a recycle delay of 5 s were used. ^{29}Si and ^{13}C chemical shifts were determined relative to the external standards Q_8M_8 and adamantane, respectively and are given with respect to the standard TMS ($\delta = 0$ ppm).

3. Results and discussion

In the following, we report on the synthesis and characterization of a series of new preceramic polymers based on phenyl-substituted silylcarbodiimides and their thermal transformation to carbon-rich SiCN ceramics. The thermal stability of the resulting SiCN materials in terms of decomposition and crystallization is a further topic addressed here.

Four different preceramic polymers S1–S4 (see Table 1) were synthesized according to Scheme 1.

The polymers appeared as rubber-like (S1), solid (S3) or viscous liquids (S2 and S4). As shown by the elemental analysis data, the polymers still contain residual chlorine due to Si–Cl

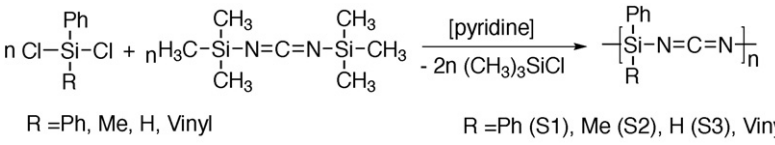

Scheme 1. Synthesis of precursors S1–S4.

end-groups and some remaining trimethylchlorosilane, as well as oxygen contamination.

The thermal transformation of the precursor polymers to SiCN ceramics was studied by means of thermogravimetry/mass spectrometry, FT-IR, Raman and solid-state NMR spectroscopy, XRD, and elemental analysis. In this context, the structural changes during thermolysis are reported representatively for samples S1 and S2, thermolyzed at different temperatures between 200 and 1000 °C. Likewise, XRD, elemental analysis and thermogravimetric measurements were performed for the characterization of the structure and morphology of the SiCN ceramics subsequently annealed between 1100 and 2000 °C.

3.1. Investigation of precursor thermolysis up to 1000 °C

3.1.1. Thermogravimetric analysis

Fig. 1 depicts the thermogravimetric (TGA) curves of polymers S1–S4 between room temperature and 1400 °C. For comparison, the TGA curves of poly(dimethylsilylcarbodiimide) S5 without phenyl substituents at the silicon atom is also given. This polymer was synthesized by analogy with the samples S1–S4, i.e. reaction of dimethyldichlorosilane with bis(trimethylsilyl)carbodiimide in the presence of pyridine.

The derived ceramic yields are 40.12%, 25.73%, 41.17% and 42.67% for samples S1, S2, S3 and S4, respectively, and reflect a special position for precursor polymer S2. Two different types of polymers can be distinguished, namely S1 and S2, which do not have cross-linkable groups, and S3 and S4, which can be cross-linked by means of dehydrocoupling- and vinyl polymerization reactions, respectively. From a comparison of polymers S1 and S2 with S5 (S5 ceramic yield 0%), all three without cross-linkable groups, it can be concluded that an increasing carbon content is accompanied by an increase of the ceramic yield in the same direction (S5 –$(SiMe_2–NCN)_n$– < S2 –$(SiPhMe–NCN)_n$– < S1 –$(SiPh_2–NCN)_n$–).

Selected mass spectrometric data are provided in Annex 1 (see Electronic Annex 1 in the online version of this article). All samples release trimethylchlorosilane and its decomposition fragments (m/z = 93, 94, 95 and 108) between 180 and 400 °C.

Table 1
Chemical structure and elemental composition of the synthesized preceramic polymers S1–S4, –$(PhSiR–N=C=N)_n$–.

Precursor	Substituent R	Composition[a]
S1	Phenyl	$Si_1C_{12.14}N_{1.81}H_{10.07}Cl_{0.19}O_{0.14}$
S2	Methyl	$Si_1C_{7.93}N_{1.83}H_{8.71}Cl_{0.12}$
S3	H	$Si_1C_{6.81}N_{1.96}H_{6.68}Cl_{0.03}O_{0.03}$
S4	Vinyl	$Si_1C_{8.75}N_{1.37}H_{8.63}Cl_{0.54}O_{0.08}$

[a] Determined from elemental analysis.

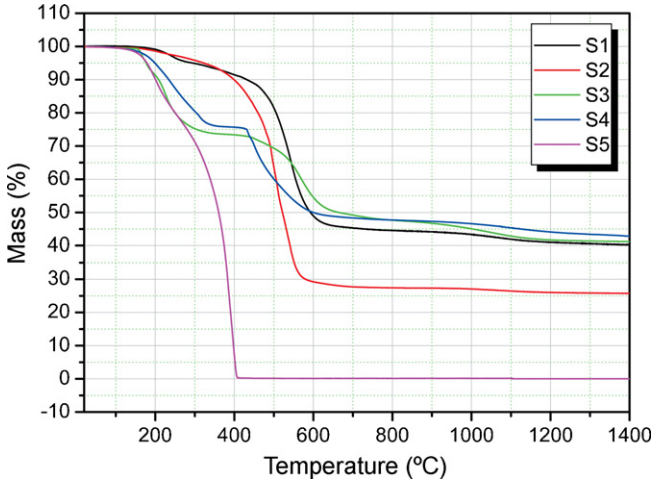

Fig. 1. Thermogravimetric curves of polymers S1–S4 and S5 –$(SiMe_2–NCN)_n$– up to 1400 °C.

For sample S1, the first mass loss takes place through reaction of trimethylsilyl-end groups and remaining chlorine atoms, followed by further polymerization.

In the case of S3 a significant amount of H_2, HCN, C_2N_2 and PhCN are also released between 200 and 400 °C. Sample S3 liberates oligomers and their fragments and undergoes dehydrocoupling reaction as indicated by the evolution of hydrogen. Between approximatively 400 and 600 °C a second thermal reaction occurs which is characterized by elimination of benzene (m/z = 78), nitriles (HCN m/z = 27, MeCN m/z = 41, PhCN m/z = 103), hydrogen (m/z = 2), methane (m/z = 16) and cyanogen C_2N_2 (m/z = 52). The temperature of evolution of gaseous C_2N_2 corresponds with the temperature of transformation of the precursor into amorphous ceramic silicon nitride (a-Si_3N_4) (T_{S1} = 556.89 °C, T_{S2} = 544.96 °C, T_{S3} = 573.14 °C and T_{S4} = 525.58 °C). Finally, a third mass loss takes place between 1000 and 1200 °C which includes release of hydrogen (m/z = 2) and small amounts of nitrogen (m/z = 28).

The evolution of the gaseous decomposition products takes place at different temperatures for each polymer. In the case of poly(methylphenylsilyl)carbodiimide S2, hydrogen (m/z = 2) and HCN (m/z = 27) are released even up to 1400 °C.

3.1.2. Solid-state NMR spectroscopy

3.1.2.1. Polymer S1. The precursor polymer S1 is a rubber-like material. Although the sample was spun at 5 kHz, the corresponding ^{29}Si and ^{13}C NMR spectra exhibit broader lines than reported in earlier studies of polysilylcarbodiimide polymers[1,10,20]. These observations might be related to some reduction of the polymer mobility due to some steric interactions in connection with the bulky phenyl groups. It is known

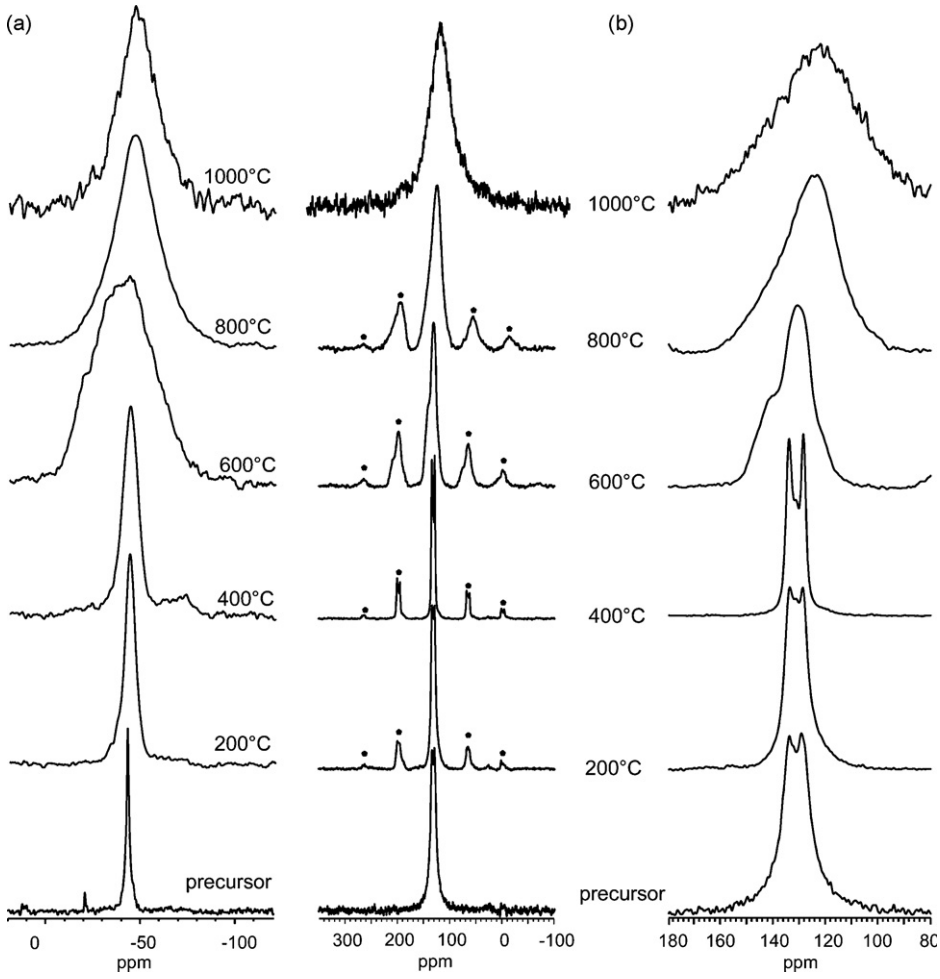

Fig. 2. Solid-state ^{29}Si (a) and ^{13}C (b) NMR spectra of precursor polymer S1 and the pyrolysis products at 200, 400, 600, 800 (CP and sample spinning rate: 5 kHz) and 1000 °C (SP and sample spinning rate: 5 kHz).

that the electronic properties of the NCN group in carbodiimides are comparable to those of the oxygen atom in polysiloxanes,[21] and the ^{29}Si NMR chemical shifts are therefore similar to those of polysiloxanes. This is supported by the ^{29}Si chemical shift values for polymer S1, which are very close to the values reported for polysiloxanes bearing the same substituents.[22]

Therefore, in the ^{29}Si{^{1}H}CP-NMR spectrum of polymer S1 (Fig. 2a) the main peak at −43.8 ppm and the small signal at −20.8 ppm are assigned to $(Ph)_2Si(NCN)_2$ sites and terminal $Si(Ph)_2Cl$ groups, respectively.[23] The presence of latter Cl-containing groups points to an incomplete exchange reaction, in agreement with the aforementioned elemental analysis data.

The ^{13}C{^{1}H} CP-NMR spectrum (see Fig. 2b) shows a broadened signal in the aromatic region with three resolvable resonances. The components at 128 and 134 ppm are related to aromatic carbons in meta and ortho positions, respectively, while the signal at about 130 ppm is a superposition due to carbons in para position and carbons directly bonded to silicon. The ^{13}C NMR signal of the NCN unit is usually less intense and occurs at around 120–124 ppm.[1,10,24] In the present case it is completely obscured by the signals of the phenyl ring carbons.

Despite the significant broadening, the main peak at −43.8 ppm is still present in the ^{29}Si {^{1}H} NMR spectra of samples annealed at 200 and 400 °C, indicating that the polymeric backbone is mostly unchanged at these temperatures. At the same time, the peak of the terminal $Si(Ph)_2Cl$ group disappears after thermolysis at 200 °C. The respective ^{13}C{^{1}H} CP-NMR spectra (see Fig. 2b) exhibit spinning side bands, reflecting an increase in chemical shift anisotropy, most probably due to a reduction in sample mobility.

Significant changes are observed in the ^{29}Si{^{1}H} and ^{13}C{^{1}H} CP-NMR spectra after sample annealing at 600 °C. The modifications are due to the decomposition of the polymer, as clearly shown by the TGA curves (see Fig. 1). The ^{29}Si{^{1}H} CP-NMR spectrum is dominated by a broad signal ranging from about −70 to −10 ppm which reflects a distribution of different $SiC_x(CN)_yN_z$ sites.[24,25] A single broadened ^{13}C resonance is detected around 131 ppm at this temperature, suggesting that cleavage of the Si–C bond and the concomitant decomposition/rearrangement of the basic polymer structure has taken place. In addition, new shoulder-like signal appears at about 120 and 140 ppm whose assignment is discussed further below.

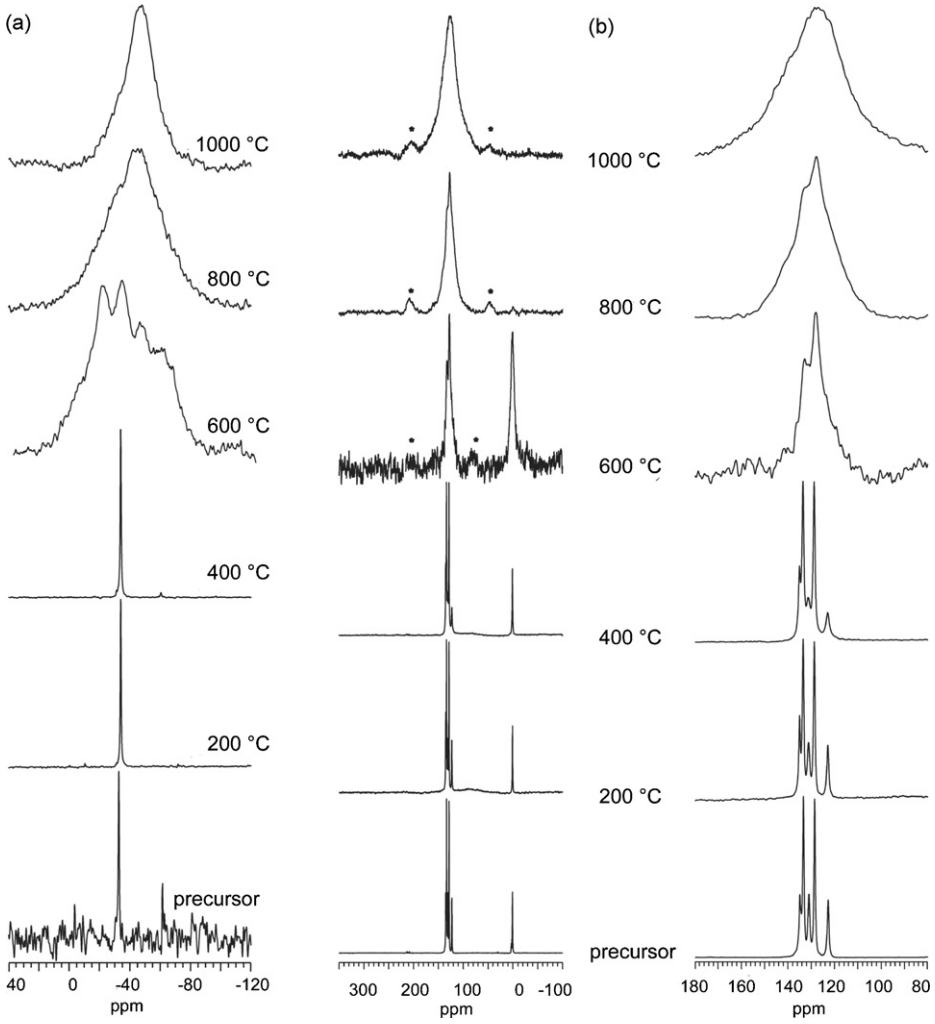

Fig. 3. Solid-state ^{29}Si (a) and ^{13}C (b) NMR spectra of precursor polymer S2 and the thermolysis products at 200, 400 (SP and sample spinning rate: 3 kHz), 600, 800 and 1000 °C (CP and sample spinning rate: 6 kHz).

Thermolysis at 800 °C is accompanied by a complete disintegration of the carbodiimide group. The ^{29}Si{^{1}H} CP-NMR spectrum is characterized by a broad and symmetric peak centered at −49 ppm, characteristic of SiN_4 units and the formation of an amorphous silicon nitride phase, which also remains for the sample annealed at 1000 °C. The respective ^{13}C{^{1}H} CP-NMR spectrum for the sample annealed at 800 °C is dominated by a broad peak centered at about 124 ppm. It shows a low field tail due to a residual signal component at 140 ppm which after thermolysis at 1000 °C disappears or is obscured by the dominant signal at 124 ppm.

The occurrence of the latter ^{13}C NMR signals after thermolysis at high temperature (≥600 °C) is a common feature of many silicon-based PDC ceramics. It reflects sp^2 carbon and is attributed to the formation of a graphene-like carbon phase. Signals with chemical shifts between 120 and 130 ppm[26–30] or at 140 ppm[31,32] were both reported in the literature, and were assigned to graphene-like phases. Sample S1 behaves differently, since signal components with both chemical shift values are observed simultaneously. The signal at 140 ppm is visible in the spectra of samples thermolyzed at 600 and 800 °C, while a resonance at 124 ppm can be registered after treatment at 800 and 1000 °C. It is worthwhile to note that two carbon signals at 119 and 141 ppm were also detected in SiBCN ceramics at a thermolysis temperature of 600 °C.[33] In that case the signals were associated with nitrogen containing graphene-like structure where carbon atoms are bonded to either carbons or nitrogen. Similar findings were reported for amorphous carbon nitride films.[34] The two signal components in the ^{13}C NMR spectrum of sample S1 are therefore attributed to the formation of a nitrogen containing sp^2 carbon phase, where the carbon species with carbon–nitrogen and carbon–carbon bonds are reflected by the resonances at 140 and 124 ppm, respectively.

3.1.2.2. Polymer S2. The most striking feature of the ^{29}Si and ^{13}C NMR spectra of precursor S2 are the very narrow and well-resolved peaks, even at low spinning speeds (3 kHz), which indicate a substantial higher mobility as compared to precursor S1. These narrow lines remain present even after pyrolysis at 400 °C. The assumed high molecular mobility most likely stems from the presence of short polymer chains and/or less interactions between the chains.

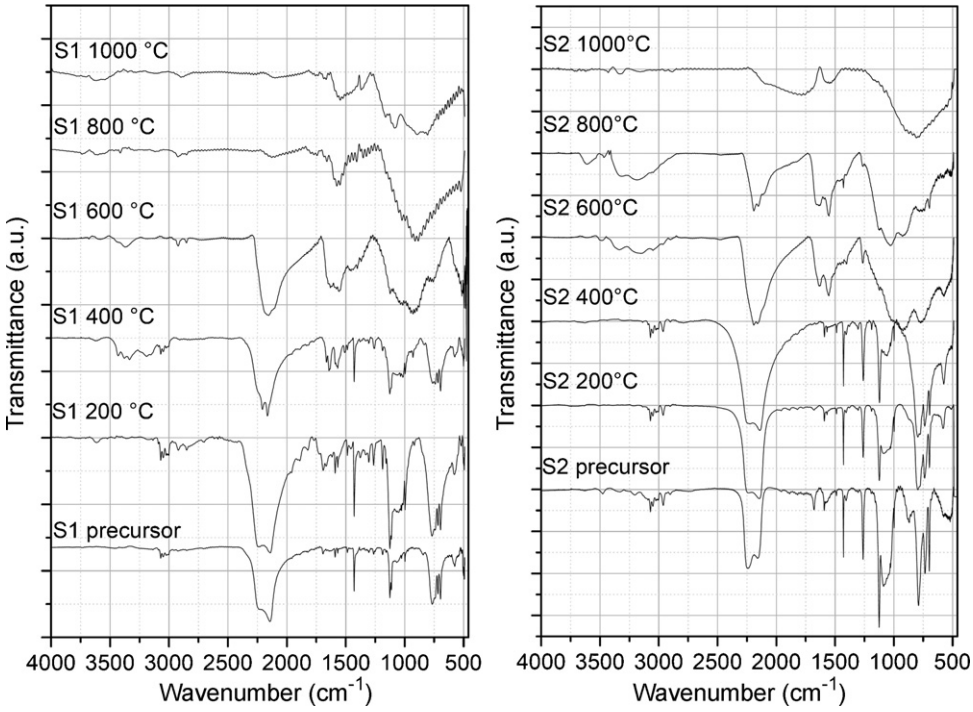

Fig. 4. FT-IR spectra of the thermolysis products of precursor systems S1 and S2 at r.t., 200. 400, 600, 800 and 1000 °C.

The ^{29}Si SP NMR spectrum of precursor S2 (see Fig. 3a) shows one signal at −32.8 ppm, which can be assigned to (CH_3)PhSi–NCN units. As expected, the ^{13}C SP NMR spectrum (Fig. 3b) contains signals in the sp^3 and in the sp^2 region. In the aliphatic region a strong signal at 0.62 ppm is visible, ascribable to the methyl group in the (CH_3)PhSi–NCN unit.

The ^{13}C NMR signal of the NCN unit, which could not be detected in sample S1 because of the significant line broadening, appears for sample S2 as a sharp, intense line at 122.8 ppm. The signal intensity decreases and the line broadens after annealing at 400 °C, while at a higher temperature it is most likely obscured by the peak of the aromatic substituent. In the low field region (128–135 ppm) the expected resonances of the aromatic carbons in ortho (134.4 ppm), meta (128.6 ppm) and para (131 ppm) position, or directly bonded to silicon (134.9 ppm) are registered. It should be mentioned that the assignment of the latter two signals is not unequivocal.

In agreement with the TGA analyses (see Fig. 1), the polymer decomposition starts at 600 °C. Indeed, at this temperature a broad resonance, ranging from 0 to −80 ppm, dominates the ^{29}Si{^{1}H} CP-NMR spectrum. Three components at −20, −31 and −44 ppm are clearly distinguished, which – according to the literature – are characteristic for $CH_3Si(–N<)_3$ and/or $SiC_2(NCN)_2$, $CH_3Si(–N<)_2(NCN)$ and $CH_3Si(–N<)(NCN)_2$ silicon sites.[1,10,21] Unlike sample S1 with silicon which exists exclusively as SiN_4 units, sample S2 shows at 800 °C also an intense ^{29}Si component, related to SiC_xN_{4-x} ($x = 1$ or 2) units.

A broadening of the aliphatic (1 ppm) and aromatic ^{13}C signals (128–133 ppm) is registered with increasing pyrolysis temperature. At the same time, the resonance at 140 ppm, due to aromatic carbons with carbon–nitrogen bonds (see above), shows up as a shoulder after thermolysis at 800 °C. As for sample S1, a single broad resonance (126 ppm) reflecting the formation of graphene-like carbon phase dominates the ^{13}C SP NMR spectrum at 1000 °C.

3.1.3. FT-IR spectroscopy

FT-IR spectra of the precursor polymers S1 and S2 along with their thermolysis products obtained at 200, 400, 600, 800 and 1000 °C are shown in Fig. 4. The FT-IR spectra recorded for the samples annealed at 200 and 400 °C are nearly the same as that of the polymer. However, the NCN band becomes somewhat broader, and in the case of S1, the bands at 2926 and 2854 cm^{-1} due to the C–H asymmetric and symmetric stretching vibrations disappear, indicating a loss of CH_3 end-groups. At the same time for S1, the Si–Cl stretching vibration at 542 cm^{-1} vanishes. Moreover, in the spectrum of S1, from room temperature to 400 °C, a raise in the intensity of the conjugated C=C bonds stretching vibration at 1693 cm^{-1} is observed. This band reflects a polyaromatic-like conjugation and its intensity increases with the temperature of annealing. In the case of S2, no band corresponding to a polyaromatic-like conjugation was found. As already discussed in the NMR part, the precursor has a liquid-like behavior and high-mobility and these properties are explained by the absence of the interactions/conjugations between the aromatic substituents.

The broad bands corresponding to C–H, NCN, conjugated C=C bonds, Si–N and Si–NCN are shown for S1 and S2 at 600 °C. For S2 at 600 °C, the symmetric deformation vibration of Si–CH_3 at 1261 cm^{-1} is still present. The band at 1642 cm^{-1} emerges in the spectrum of S1 at 600 °C and at 1678 cm^{-1} for S2 at 600 and 800 °C. This band corresponds to a C=N stretching vibration and can be traced back to a nitrogen containing graphene-like structure,[35–37] as reported from the ^{13}C MAS

Table 2
Composition of precursor systems S1–S4 thermolyzed at 1100, 1400, 1500, 1700 and 2000 °C.

Sample	Composition (wt.%)				Empirical formula normalized on Si
	Si	C	N	O	
S1 1100 °C	21.80	60.91	16.69	0.60	$Si_1C_{6.52}N_{1.53}O_{0.05}$
S1 1400 °C	24.58	56.46	18.67	0.29	$Si_1C_{5.36}N_{1.52}O_{0.02}$
S1 1500 °C	24.05	60.19	15.47	0.29	$Si_1C_{5.84}N_{1.29}O_{0.02}$
S1 1700 °C	22.69	76.92	0.35	0.04	$Si_1C_{7.91}N_{0.03}$
S1 2000 °C	24.06	75.66	0.28	0.00	$Si_1C_{7.34}N_{0.02}$
S2 1100 °C	35.15	45.46	18.98	0.41	$Si_1C_{3.02}N_{1.08}O_{0.02}$
S2 1400 °C	32.64	46.63	19.53	1.19	$Si_1C_{3.33}N_{1.20}O_{0.06}$
S2 1500 °C	24.52	55.62	18.98	0.87	$Si_1C_{5.29}N_{1.55}O_{0.06}$
S2 1700 °C	33.76	65.77	0.46	0.00	$Si_1C_{4.44}N_{0.03}$
S2 2000 °C	32.96	66.81	0.16	0.07	$Si_1C_{4.73}N_{0.01}$
S3 1100 °C	30.93	47.52	20.98	0.52	$Si_1C_{3.59}N_{1.36}O_{0.03}$
S3 1400 °C	34.69	47.50	16.98	0.83	$Si_1C_{3.20}N_{0.98}O_{0.04}$
S3 1500 °C	29.86	57.94	12.20	0.00	$Si_1C_{4.53}N_{0.82}$
S3 1700 °C	31.23	68.34	0.44	0.00	$Si_1C_{5.11}N_{0.03}$
S3 2000 °C	33.98	66.00	0.02	0.00	$Si_1C_{4.53}N_{0.00}$
S4 1100 °C	25.38	55.62	14.20	4.80	$Si_1C_{5.11}N_{1.12}O_{0.33}$
S4 1400 °C	25.81	55.32	14.43	3.44	$Si_1C_{5.00}N_{1.12}O_{0.23}$
S4 1500 °C	23.21	69.75	6.55	0.49	$Si_1C_{7.01}N_{0.57}O_{0.04}$
S4 1700 °C	27.75	72.05	0.20	0.00	$Si_1C_{6.06}N_{0.01}$
S4 2000 °C	23.69	76.27	0.04	0.00	$Si_1C_{6.36}N_{0.00}$

NMR results part. The asymmetric stretching band of the NCN group at 2232 cm^{-1} is found in the materials S1 and S2 annealed up to 800 °C. Nevertheless, between 600 and 800 °C the intensity of NCN band diminishes more significantly for sample S1 than for sample S2, indicating a different mechanism of the thermal transformation. After heat treatment beyond 800 °C, the N–H stretching band at 3400 cm^{-1} and N–Si–N stretching band at 800 cm^{-1} (SiN_4 unit) show up. At the same time, the phenylic C–H stretching band decreases significantly in intensity. In the amorphous ceramics S1 and S2 obtained at 1000 °C the vibration bands corresponding to Si–N (~800 cm^{-1}), C=C (carbon-free) (~1550 cm^{-1}) and N–H (~3550 cm^{-1}) were assigned as the most prominent signals. In summary, the experimental findings obtained from the FT-IR investigations are completely consistent with the aforementioned solid-state NMR data.

3.2. Investigation of precursor thermolysis above 1000 °C

3.2.1. Elemental analysis

Table 2 shows the elemental compositions of the amorphous SiCN ceramics as derived from the preceramic polymers S1–S4 after pyrolysis at 1100, 1400, 1500, 1700 and 2000 °C.

The amount of carbon in the SiCN ceramics is controlled by the initial carbon amount in the polymers, as shown in Fig. 5. It is seen that the precursor polymers have compositions prior to thermal treatment, which lie almost perfectly on the tie-line between Si_3N_4 and C. The SiCN ceramics obtained from the present phenyl-containing polysilylcarbodiimides S1–S4 are definitely carbon-rich materials. This is indicated in Fig. 5 by the area marked in blue, which reflects the compositional range of the amorphous ceramics obtained so far by other polysilylcarbodiimide-derived SiCN ceramics.[13,16,24,38–40]

Upon thermolysis at 1100 °C the carbon content slightly decreases. The ceramic materials obtained from precursor polymers S1 and S3 remain on the tie-line, while for samples S2 and S4 a shift away from the tie-line is found. Elemental analysis composition of S2 and S4 (see Table 2) and the shift from the tie-line of these samples indicate the presence of small amounts of SiC in these materials.

By increasing the thermolysis temperature above 1500 °C, the relative content of carbon increases. From 1700 to 2000 °C

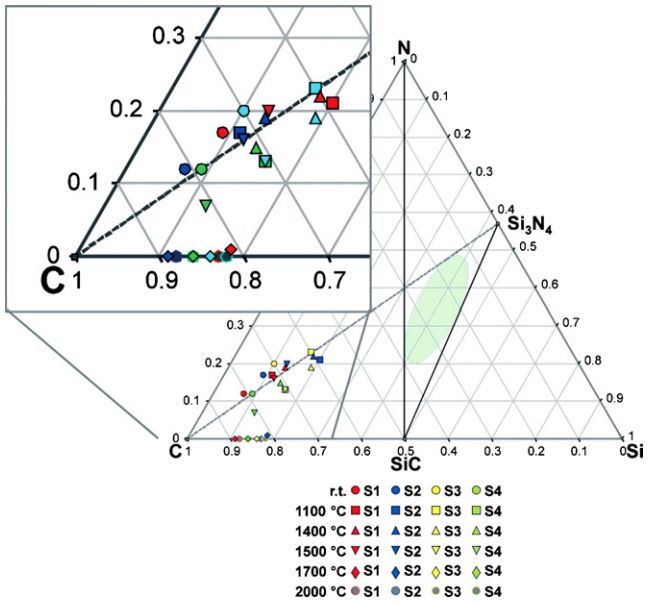

Fig. 5. Isothermal section of the ternary SiCN phase diagram with compositions analyzed for the SiCN ceramics and determined for the polymers S1–S4 by neglecting hydrogen as indicated. The blue marked area in the right part of the graph indicates typical SiCN compositions for other polysilylcarbodiimides as published in the literature.[13,16,24,38–40].

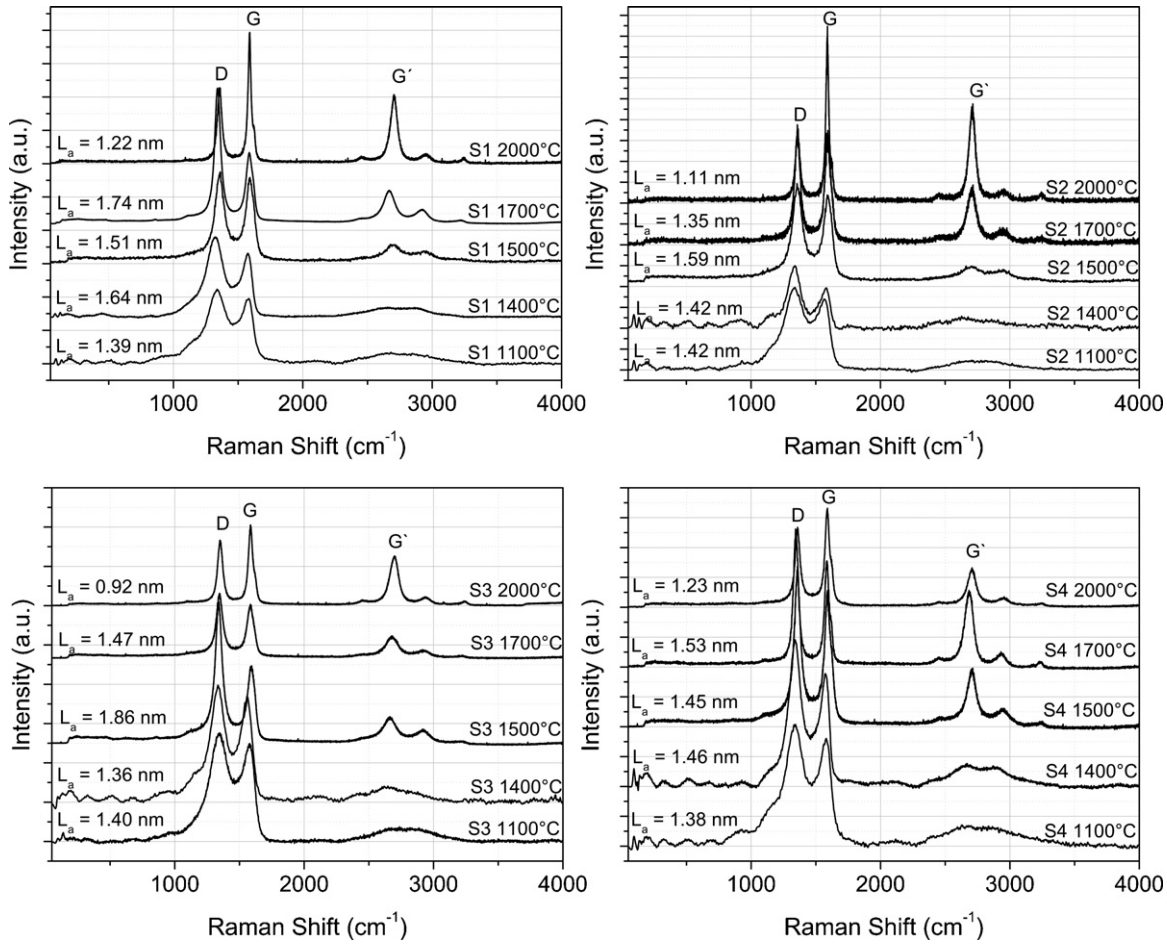

Fig. 6. Micro-Raman spectroscopy measurements of the thermolysis products of the precursor systems S1–S4 at 1100, 1400, 1500, 1700 and 2000 °C.

the composition of all the samples lies on the tie-line between SiC and C, indicating the complete loss of nitrogen after the high-temperature treatment.

3.2.2. Raman spectroscopy

Raman spectroscopy is an important nondestructive tool for the examination of the structural evolution of the free carbon phase in PDCs.[6,41–45] The most prominent features of free carbon in the Raman spectra of PDCs are the so-called disorder-induced "D- and D′ bands" at approx. 1350 and 1620 cm^{-1}, the "G band" at approx. 1582 cm^{-1} due to in-plane bond stretching of sp^2 carbon, as well as the G′ band (the overtone of the D band which is always observed in defect-free samples at 2700 cm^{-1}).[41–45] Another Raman feature at about 2950 cm^{-1}, associated with a D + G combination mode and induced by disorder, is observed in the spectrum of carbon as well.

In the case of an amorphous carbon phase, the D and G bands can vary in intensity, position and width, depending on the structural organization of the sample under investigation. The intensity ratio of the D and G modes, $I(D)/I(G)$, enables the evaluation of the carbon cluster size by using the formula reported by Ferrari and Robertson[41]:

$$\frac{I(D)}{I(G)} = C'(\lambda)L_a^2$$

where, L_a is the size of carbon domains along the sixfold ring plane (lateral size), and C' is a coefficient that depends on the excitation wavelength of the laser. The value of the coefficient C' for the wavelength of 514.5 nm of the Ar-ion laser employed here is 0.0055 $Å^{-2}$. Gaussian–Lorentzian curve fitting of the Raman bands was performed in order to extract the $I(D)/I(G)$ intensity ratios and to determine the size of the free carbon cluster formed in the S1–S4 ceramics. Because of the strong fluorescence of the samples thermolyzed at lower temperatures, Raman studies were only performed for the samples which were heated to 1100 °C and above.

Raman spectra of samples S1–S4 thermolyzed at 1100, 1400, 1500, 1700 and 2000 °C are presented in Fig. 6. From 1100 to 1500 °C, the ceramics S1–S4 exhibit broad signals and strong overlap as a consequence of the pronounced structural disorder of the carbon phase. At 1700 °C, very distinct and narrow peaks of D and G modes are observed due to a more ordered graphite-like structure (graphene layers). At 2000 °C, turbostratic carbon is formed, as indicated primarily by the increase in the intensity of the G band and the concomitant decrease of the D band, and additionally by the overtone band profile.

Unexpectedly, the $I(D)/I(G)$ ratio remains almost constant with values higher than 1 for S1–S4 between 1100 and 1700 °C and decreases to values less than 1 after annealing at 2000 °C. The decrease in $I(D)/I(G)$ and consequently in the cluster size

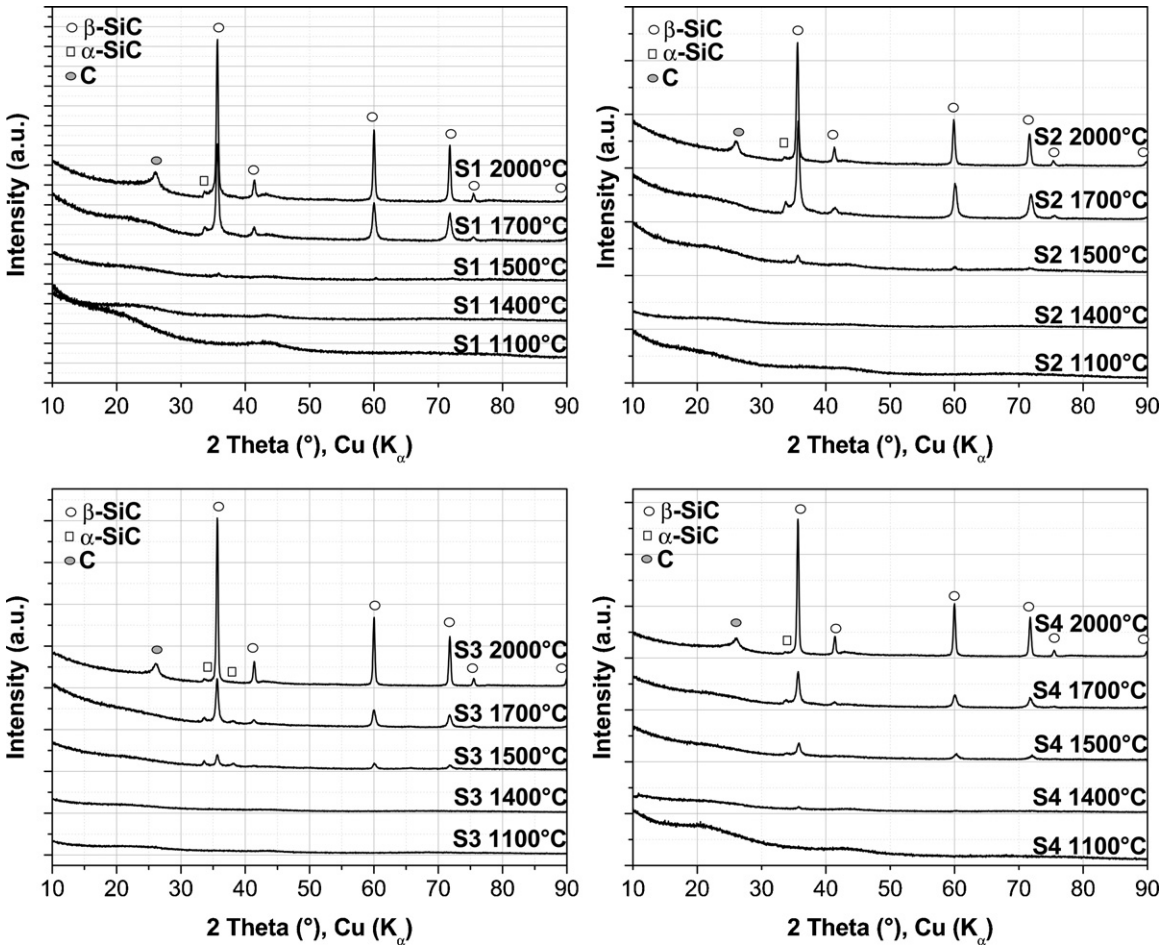

Fig. 7. X-ray diffractograms of the thermolysis products obtained from S1 to S4 at 1100, 1400, 1500, 1700 and 2000 °C.

for the samples annealed at 2000 °C is traced back to a higher organization of the C sp^2 layers. At this temperature, the smallest carbon cluster size (0.92–1.23 nm) is analyzed and this feature is traced back to the formation of turbostratic carbon as will be shown in the XRD part below.

The second-order G′ band, corresponding to the overtone of the D band, appears in the range of 2500–2800 cm^{-1} and is always observed in defect-free samples. The G′ band is very sensitive to the stacking order of the graphene sheets along the *c* axis.[45] As shown in Fig. 6, the shape of G′ band changes with the temperature of thermolysis and this behavior is associated with the degree of graphitization of the samples. In the case of turbostratic carbon, there is no stacking order between adjacent layers and therefore there is a very weak interaction between the graphene planes so that turbostratic carbon can be considered to be 2D graphite, similar to a graphene layer. The 2D carbon can be fit by one Gaussian–Lorentzian peak and the 3D carbon with two or more peaks. The spectra of samples S1–S4 show no defined G′ bands up to 1400 °C and even 1500 °C (for S1–S3) indicate the high degree of disorder at these temperatures. From 1700 to 2000 °C, a sharp and well-defined G′ band, fitted by a single Gaussian–Loretzian peak is observed. The G′ band single band provides direct experimental evidence that the turbostratic carbon phase of S1–S4 can be considered as 2D graphite. The increase in intensity of G′ relative to the intensity of D band, indicates the enhancement in the structural organization of the carbon. Moreover, the G′ band for S1 and S2 at 2000 °C is more intense than the D band.

The enhancement in the organization and in the formation of a defect-free structure of carbon phase is also shown by the decrease of the intensity of D + G combination band at about 2950 cm^{-1} with the temperature of thermolysis in all four samples.

3.2.3. X-ray diffraction

The crystallization behavior of the SiCN ceramics derived from precursor systems S1–S4 was studied by X-ray diffraction (Fig. 7). In contrast to the previous studies on polysilylcarbodiimide-derived ceramics, no crystalline Si_3N_4 phases were detected in our systems.

The ceramics S2–S4 are amorphous up to 1500 °C when a fraction of amorphous Si_3N_4 transforms to crystalline SiC. At this temperature, the composition can be expressed as a mixture of three phases comprising of a-Si_3N_4, a-C and α- and β-SiC. As reported by Iwamoto et al., a significant amount of carbon can hinder the crystallization of amorphous Si_3N_4 as shown by solid-state NMR and X-ray diffraction analysis.[14] Contrary to samples S2–S4, the sample with the highest carbon content, S1,

remains amorphous even beyond 1500 °C. The separation of β-SiC was detected at 1700 °C. This finding is directly correlated to the free amount of carbon which stabilizes the ceramic structure against crystallization. At $T \geq 1700$ °C samples S1–S4 crystallize to yield β-SiC and small fraction of α-SiC, while at 2000 °C the presence of turbostratic carbon is also detected.

Furthermore, in spite of the different molecular structure and carbon content, samples S2–S4 show the same crystallization behavior. Only sample S1 with the highest carbon content remains amorphous up to higher temperature as compared to the samples S2–S4. At 1500 °C, samples S2–S4 start to crystallize to give α- and β-SiC, while the remaining Si_3N_4 phase persists to be amorphous. At 2000 °C, the clusters of crystalline α- and β-SiC are embedded in the matrix of turbostratic carbon.

4. Conclusions

The present study demonstrates that the C/Si ratio of PDCs can be effectively controlled by the design and synthesis of organosilicon precursors. Phenyl substituents at Si in polysilylcarbodiimides allow the formation of carbon-rich SiCN ceramics. It was also found that different substituents attached to the silicon atoms confer different mechanisms of thermal transformation. In addition to thermal gravimetric analysis, the thermolysis of novel phenyl-containing polysilylcarbodiimides was investigated by means of solid-state NMR and FT-IR spectroscopy.

The intrinsically high carbon content seals off the amorphous silicon nitride domains leading to an enhanced thermal stability of the SiCN ceramics with respect to crystallization. Moreover, due to the high amount of carbon in our samples, the crystallization of silicon nitride was inhibited. Graphene layers seal the amorphous Si_3N_4 and prevent the out diffusion of nitrogen and therefore increase the stability of Si_3N_4 clusters. The C-rich SiCN proves to be more temperature resistant than that of the published SiCN ceramics with lower C-content. For instance, the crystallization of poly(diphenylsilylcarbodiimide) occurs at 50 °C higher than that of the reported SiCN ceramics derived from other polysilylcarbodiimides.[15]

The carbon-rich SiCN ceramics investigated in our study crystallize directly to α- and β-SiC. The formation of crystalline silicon nitride was not observed.

In conclusion, carbon-rich SiCN ceramics are excellent candidate materials for high-temperature applications. The effect of carbon on the oxidative stability of carbon-rich SiCN ceramics is currently under investigation.

Acknowledgments

The authors acknowledge the Deutsche Forschungsgemeinschaft, Bonn, Germany (DFG-NSF research initiative) and the Fonds der Chemischen Industrie, Frankfurt (Germany) for their financial support. G.M. and R.R. thank Claudia Fasel for the STA measurements.

Appendix A. Supplementary data

Supplementary data associated with this article can be found, in the online version, at doi:10.1016/j.jeurceramsoc.2009.03.026.

References

1. Riedel, R., Mera, G., Hauser, R. and Klonczynski, A., Silicon-based polymer-derived ceramics: synthesis properties and applications—a review. *J. Ceram. Soc. Jpn.*, 2006, **114**(6), 425–444.
2. Mera, G. and Riedel, R., Organosilicon-based polymers as precursors for ceramics. In *Polymer Derived Ceramics*, DEStech Publications, Inc., Lancaster, PA, USA, 2009, pp. 50–88, in press.
3. Kleebe, H.-J., Blum, Y. D. and MacQueen, D. B., SiOC ceramic with high excess free carbon. *J. Eur. Ceram. Soc.*, 2008, **28**(5), 1037–1042.
4. Kleebe, H.-J., Gregori, G., Babonneau, F., Blum, Y. D., MacQueen, D. B. and Masse, S., Evolution of C-rich SiOC ceramics—part I. Characterization by integral spectroscopic techniques: solid-state NMR and Raman spectroscopy. *Int. J. Mater. Res.*, 2006, **97**(6), 699–709.
5. Gregori, G., Kleebe, H.-J., Blum, Y. D. and Babonneau, F., Evolution of C-rich SiOC ceramics—part II. Characterization by high lateral resolution techniques: electron energy-loss spectroscopy, high-resolution TEM and energy-filtered TEM. *Int. J. Mater. Res.*, 2006, **97**(6), 710–720.
6. Saha, A., Raj, R., Williamson, D. L. and Kleebe, H.-J., Characterization of nanodomains in polymer-derived SiCN ceramics employing multiple techniques. *J. Am. Ceram. Soc.*, 2005, **88**(1), 232–234.
7. Störmer, H., Kleebe, H.-J. and Ziegler, G., Metastable SiCN glass matrices studied by energy-filtered electron diffraction pattern analysis. *J. Non-Cryst. Solids*, 2007, **353**, 2867–2877.
8. Hörz, M., Zern, A., Berger, F., Haug, J., Müller, K., Aldinger, F. and Weinmann, M., Novel polysilazanes as precursors for silicon nitride/silicon carbide composites without "free" carbon. *J. Eur. Ceram. Soc.*, 2005, **25**, 99–110.
9. Hurwitz, F. I., Heimann, P., Farmer, S. C. and Hembree Jr., D. M., Characterization of the pyrolytic conversion of polysilsesquioxanes to silicon oxycarbides. *J. Mater. Sci.*, 1993, **28**, 6622–6630.
10. Hurwitz, F. I., Heimann, P. J. and Kacik, T. A., Redistribution reactions in Blackglas™ during pyrolysis and their effect on oxidative stability. *Ceram. Eng. Sci. Proc.*, 1995, **16**, 217.
11. Turquat, C., Kleebe, H.-J., Gregori, G., Walter, S. and Soraru, G. D., TEM and EELS study of non-stoichiometric SiCO glasses. *J. Am. Ceram. Soc.*, 2001, **84**, 2189–2196.
12. Raj, R., Riedel, R. and Soraru, G. D., Introduction to the special topical issue on ultrahigh-temperature polymer-derived ceramics. *J. Am. Ceram. Soc.*, 2001, **84**(10), 2158–2159.
13. Riedel, R., Kroke, E., Greiner, A., Gabriel, A. O., Ruwisch, L. and Nicolich, J., Inorganic solid state chemistry with main group element carbodiimides. *J. Chem. Mater.*, 1998, **10**, 2964–2979.
14. Iwamoto, Y., Völger, W., Kroke, E. and Riedel, R., Crystallization behavior of amorphous Si–C–N ceramics derived from organometallic precursors. *J. Am. Ceram. Soc.*, 2001, **84**(10), 2170–2178.
15. Klebe, J. F. and Murray, J. G., *Organosiliconcarbodiimide polymers and process for their preparation*. US Patent 3352799, 14 November 1967.
16. Kumar, P. and Shankar, R., Thermal studies on oligosilylbiguanides: a mechanistic approach. *Silicon Chem.*, 2002, **1**, 233–237.
17. Vostokov, I. A., Dergunov, Y. I. and Gordetsov, A. S., Reaction of organosilicon, organogermanium, and organotin compounds with dicyanodiamide. New method for obtaining organoelemental carbodiimides. *Zh. Obshch. Khim.*, 1977, **47**(8), 1769–1771.
18. Shriver, D. F. and Drezdzon, M. A., *The Manipulation of Air-sensitive Compounds* (*2nd ed.*). Wiley, New York, 1986.
19. Metz, G., Xiaoling, W. and Smith, S. O., Ramped-amplitude cross polarization in magic-angle-spinning NMR. *J. Magn. Res. Ser. A*, 1994, **110**, 219–227.

20. Schuhmacher, J., Weinmann, M., Bill, J., Aldinger, F. and Müller, K., Solid state NMR studies of the preparation of Si–C–N ceramics from polysilylcarbodiimide polymers. *Chem. Mater.*, 1998, **10**, 3913–3922.
21. Schädler, H.-D., Jäger, L. and Senf, I., Pseudoelementverbindungen V. Pseudochalkogene—versuch der empirischen und theoretischen Charakterisierung. *Z. Anorg. Allg. Chem.*, 1993, **619**, 1115–1120.
22. Gädda, T. M. and Weber, W. P., Polydiphenylsiloxane–polydimethylsiloxane–polydiphenylsiloxane triblock copolymers. *J. Polym. Sci. Part A: Polym. Chem.*, 2006, **44**(11), 3629–3639.
23. Marsmann, H., *29Si-NMR Spectroscopic Results, NMR*. Springer, Grundlagen und Fortschritte, 1981.
24. Gabriel, A. O., Riedel, R., Dressler, W., Reichert, S., Gervais, C., Maquet, J. and Babonneau, F., Thermal decomposition of poly(methylsilsesquicarbodiimide) to amorphous Si–C–N Ceramics. *Chem. Mater.*, 1999, **11**, 412–420.
25. Riedel, R., Greiner, A., Miehe, G., Dressler, W., Fuess, H., Bill, J. and Aldinger, F., The first crystalline solids in the ternary Si–C–N system. *Angew. Chem., Int. Ed. Engl.*, 1997, **36**, 603–606.
26. Berger, F., Weinmann, M., Aldinger, F. and Müller, K., Solid-state NMR studies of the preparation of Si–Al–C–N ceramics from aluminum-modified polysilazanes and polysilylcarbodiimides. *Chem. Mater.*, 2004, **16**, 919–929.
27. Schuhmacher, J., Berger, F., Weinmann, M., Bill, J., Aldinger, F., Müller, K. and Solid-state, N. M. R., FT-IR studies of the preparation of Si–B–C–N ceramics from boron-modified polysilazanes. *Appl. Organomet. Chem.*, 2001, **15**, 809–819.
28. Soraru, G. D., Babonneau, F. and Mackenzie, J. D., Structural evolutions from polycarbosilane to SiC ceramic. *J. Mater. Sci.*, 1990, **9**, 3886–3893.
29. Bois, L., Maquet, J., Babonneau, F., Mutin, P. H. and Bahloul, D., Structural characterization of sol–gel derived oxycarbide glasses. 1. Study of the pyrolysis process. *Chem. Mater.*, 1994, **6**, 796–802.
30. Gerardin, C., Tauelelle, F. and Bahloul, D., Pyrolysis chemistry of polysilazane precursors to silicon carbonitride. *J. Mater. Chem.*, 1997, **7**, 117–126.
31. Lewis, R. H. and Maciel, G. E., Magnetic resonance characterization of solid-state intermediates in the generation of ceramics by pyrolysis of hydridopolysilazane. *J. Mater. Sci.*, 1995, **30**, 5020–5030.
32. Gervais, C., Babonneau, F., Ruwisch, L., Hauser, R. and Riedel, R., Solid-state NMR investigations of the polymer route to SiBCN ceramics. *Can. J. Chem.*, 2003, **81**, 1359–1369.
33. Sehlleier, Y. H., Verhoeven, A. and Jansen, M., NMR studies of short and intermediate range ordering of amorphous Si–B–N–C–H pre-ceramic at the pyrolysis stage of 600 °C. *J. Mater. Chem.*, 2007, **17**, 4316–4319.
34. Gammon, W. J., Malyarenko, D. I., Kraft, O., Hoatson, G. L., Reilly, A. C. and Holloway, B. C., Hard and elastic amorphous carbon nitride thin films studied by ^{13}C nuclear magnetic resonance spectroscopy. *Phys. Rev. B*, 2002, **66**, 153402-1–153402-4.
35. Socrates, G., *Infrared and Raman Characteristic Group Frequencies: Tables and Charts*. Wiley & Sons, 2004, Auflage 0003.
36. Kaufman, J. H., Metin, S. and Saperstein, D. D., Symmetry breaking in nitrogen-doped amorphous carbon: infrared observation of the Raman-active *G* and *D* bands. *Phys. Rev. B: Condens. Matter*, 1989, **39**(18), 13053–13060.
37. Bouchet-Fabre, B., Marino, E., Lazar, G., Zellam, K., Clin, M., Ballutaud, D., Abel, F. and Godet, C., Spectroscopic study using FTIR, Raman, XPS and NEXAFS of carbon nitride thin films deposited by RF magnetron sputtering. *Thin Solid Films*, 2005, **482**, 167–171.
38. Gabriel, A. O., Riedel, R., Storck, S., Maier, W. F. and Synthesis, Thermally induced ceramisation of a polymethylsilsesquicarbodiimide-gel. *Appl. Organomet. Chem.*, 1997, **11**, 833–841.
39. Kim, D. S., Kroke, E., Riedel, R., Gabriel, A. O. and Shim, S. C., An anhydrous sol–gel system derived from methyldichlorosilane. *Appl. Organomet. Chem.*, 1999, **13**, 495–499.
40. Riedel, R. and Gabriel, A. O., Synthesis of polycrystalline silicon carbide by a liquid phase process. *Adv. Mater.*, 1999, **11**(3), 207–209.
41. Ferrari, A. C. and Robertson, J., Interpretation of Raman spectra of disordered and amorphous carbon. *Phys. Rev. B*, 2000, **61**, 14095–14107.
42. Ferrari, A. C., Meyer, J. C., Scardaci, V., Casiraghi, C., Lazzeri, M., Mauri, F., Piscanec, S., Jiang, D., Novoselov, K. S., Roth, S. and Geim, A. K., Raman spectrum of graphene and graphene layers. *Phys. Chem. Lett.*, 2006, **97**, 187401-1–187401-4.
43. Pimenta, M. A., Dresselhaus, G., Dresselhaus, M. S., Cançado, L. G., Jorio, A. and Saito, R., Studying disorder in graphite-based systems by Raman spectroscopy. *Phys. Chem. Chem. Phys.*, 2007, **9**, 1276–1290.
44. Ferrari, A. C., Raman spectroscopy of graphene and graphite: disorder, electron–phonon coupling, doping and nonadiabatic effects. *Solid State Commun.*, 2007, **143**, 47–57.
45. Cançado, L. G., Takai, K., Enold, E., Endo, M., Kim, Y. A., Mizusaki, H., Jorio, A., Coelho, L. N., Magalhaes-Paniago, R. and Pimenta, M. A., General equation for the determination of the crystallite size *La* of nanographite by Raman spectroscopy. *Appl. Phys. Lett.*, 2006, **88**, 163106-1–163106-3.